◆ Human Brain Mapping 37:4069–4083 (2016) ◆

Preserved White Matter Microstructure in Young Patients with Anorexia Nervosa?

Gerit Pfuhl,[1,2†] Joseph A. King,[1,3†] Daniel Geisler,[1,3] Benjamin Roschinski,[1] Franziska Ritschel,[1,3] Maria Seidel,[1,3] Fabio Bernardoni,[1,3] Dirk K. Müller,[4] Tonya White,[5] Veit Roessner,[1] and Stefan Ehrlich[1,3,6,7]*

[1]Eating Disorders Research and Treatment Center at the Dept. of Child and Adolescent Psychiatry, Faculty of Medicine, Technische Universität Dresden, Dresden, Germany
[2]Department of Psychology, UiT the Arctic University of Norway & Department of Psychology, Norwegian University of Science and Technology, Trondheim, Norway
[3]Division of Psychological and Social Medicine and Developmental Neurosciences, Faculty of Medicine, Technische Universität Dresden, Dresden, Germany
[4]Department of Psychiatry and Neuroimaging Center, Technische Universität Dresden, Dresden, Germany
[5]Department of Child and Adolescent Psychiatry & Department of Radiology, Erasmus University Medical Centre, Rotterdam, The Netherlands
[6]MGH/MIT/HMS Martinos Center for Biomedical Imaging, Massachusetts General Hospital, Charlestown, Massachusetts
[7]Harvard Medical School, Department of Psychiatry, Massachusetts General Hospital, Boston, Massachusetts

Abstract: A massive but reversible reduction of cortical thickness and subcortical gray matter (GM) volumes in Anorexia Nervosa (AN) has been recently reported. However, the literature on alterations in white matter (WM) volume and microstructure changes in both acutely underweight AN (acAN) and after recovery (recAN) is sparse and results are inconclusive. Here, T1-weighted and diffusion-weighted MRI data in a sizable sample of young and medication-free acAN ($n = 35$), recAN ($n = 32$), and age-matched female healthy controls (HC, $n = 62$) were obtained. For analysis, a well-validated global probabilistic tractography reconstruction algorithm including rigorous motion correction implemented in FreeSurfer: TRACULA (TRActs Constrained by UnderLying Anatomy) were used. Additionally, a clustering algorithm and a multivariate pattern classification technique to WM metrics to predict group membership were applied. No group differences in either WM volume or WM microstructure were detected with standard analysis procedures either in acAN or recAN relative to HC after controlling for the number of performed statistical tests. These findings were not affected by age, IQ, or psychiatric symptoms. While cluster analysis was unsuccessful at discriminating between groups, multivariate pattern classification showed some ability to separate acAN from HC (but not

Additional Supporting Information may be found in the online version of this article.

Contract grant sponsor: Deutsche Forschungsgemeinschaft as well as the Roland Ernst Stiftung; Contract grant numbers: EH 367/5-1 & SFB 940/1.

[†]Gerit Pfuhl and Joseph A. King contributed equally to this work.

*Correspondence to: Stefan Ehrlich, M.D.; Division of Psychological and Social Medicine and Developmental Neurosciences, Faculty of Medicine, Technische Universität Dresden, Dresden, Germany. E-mail: stefan.ehrlich@tu-dresden.De

Received for publication 5 November 2015; Revised 13 June 2016; Accepted 15 June 2016.

DOI: 10.1002/hbm.23296

Published online 12 July 2016 in Wiley Online Library (wileyonlinelibrary.com).

recAN from HC). However, these results were not compatible with a straightforward hypothesis of impaired WM microstructure. The current findings suggest that WM integrity is largely preserved in non-chronic AN. This finding stands in contrast to findings in GM, but may help to explain the relatively intact cognitive performance of young patients with AN and provide the basis for the fast recovery of GM structures. *Hum Brain Mapp 37:4069–4083, 2016.*

Key words: diffusion tensor imaging; tractography; fractional anisotropy; machine learning algorithm; anorexia nervosa

INTRODUCTION

Anorexia nervosa (AN) is a severe eating disorder that usually begins in adolescence in females and is associated with intense fear of weight gain, preoccupation with body image and emaciation [American Psychiatric Association, 2000]. AN has the largest standardized mortality ratio among all psychiatric disorders [Papadopoulos et al., 2009], but its etiology remains unknown.

In acutely underweight AN patients (acAN), a major reduction in grey matter (GM) volume [for review, see Seitz et al., 2014, 2016; Van den Eynde et al., 2012] and cortical thickness [King et al., 2015] has been observed with a possible exception of increased GM in the orbitofrontal cortex [Frank et al., 2013]. However, GM atrophy may be reversible already following partial weight restoration [Bernardoni et al., 2016; Roberto et al., 2011] and recovered AN (recAN) show no lasting major GM thickness or subcortical GM volume differences relative to age-matched healthy control participants [HC; King et al., 2015; Wagner et al., 2006]. Nonetheless, some irreversible GM damage may be expected in some patients depending on factors including age of disease onset, duration of illness and illness severity.

While less is known about changes in white matter (WM) alterations associated with AN, recent meta-analyses suggest that the general pattern of reduced GM volume in acAN and normalization following weight restoration may also be observable in WM [Seitz et al., 2014, 2016; Titova et al., 2013; see also Boghi et al., 2011; Lavagnino et al., 2015; Seitz et al., 2015] which is also supported by animal model [Reyes-Haro et al., 2015]. The largest known longitudinal study of WM volume in AN ($n = 34$) reported links between increases in body mass index (BMI) and WM volume increases [Roberto et al., 2011].

Going beyond measures of WM volume, a growing number of recent AN studies have capitalized on advances in MR technology to explore microstructural changes in WM using diffusion tensor imaging (DTI). DTI uses the translational motion of water molecules to estimate diffusion rates in three-dimensional space and is highly sensitive to subtle changes in WM integrity since water molecules show the fastest unidirectional diffusion along highly directional myelinated WM tracts [Jones et al., 2013; Le Bihan, 2003]. The most common metric of WM integrity is fractional anisotropy (FA), a scalar value of the degree of anisotropic/directional diffusion within a voxel associated with axon density and myelination. Additional measures including mean diffusivity (MD), the overall degree of water diffusion, radial diffusivity (RD), the magnitude of water molecule displacements perpendicular to WM pathways and axial diffusivity (AD), the rate of diffusion in the parallel direction may help to better specify and characterize dynamic (pathological) changes in tissue microstructure [Alexander et al., 2007].

To date, most DTI studies in AN have been based on small samples ($n < 20$) using voxel-based approaches and results have been mixed [for review, see Frank, 2015a; Martin Monzon et al., 2016]. Reduced FA has been reported in both adolesecent [Frank et al., 2013] and adult acAN [Frieling et al., 2012; Kazlouski et al., 2011; Nagahara et al., 2014; Via et al., 2014] relative to HC in multiple diffuse WM pathways including fornix, fronto-occipital fasciculus, posterior cingulum, posterior thalamic radiation, mediodorsal thalamus, superior longitudinal fasciculus, and cerebellum. However, the only consistent FA reduction reported thus far has been located in the fornix [Frank, 2015b], a WM tract particularly susceptible to artifacts in diffusion imaging [Jones and Cercignani, 2010]. Furthermore, some studies have reported regional FA increases [Frank et al., 2013]. For example, in a recent comparatively well-powered study in adolescents ($n = 22$ acAN) study, Vogel et al. [2016] found increased FA in bilateral frontal, parietal, and temporal regions.

Only two known DTI studies have focused on recAN. Yau et al. [2013] reported intact FA, but reduced MD in frontal, parietal and cingulum WM regions in a small sample of former patients. In a recent study with the largest AN sample to date ($n = 24$ recAN), Shott et al. [2015] targeted WM connections (using local probabalistic tractography) between selected regions of interest within the brain reward circuit and found greater strength of WM fiber connections, but lower FA (using voxel-based analysis) in the insula, ventral striatum, and orbitofrontal cortex.

In attempt to quantify potential alterations in WM integrity in AN in specific known pathways in greater detail than that provided by voxel-based analysis, two additional studies have also employed tractography. In a small sample of adolescent acAN, Travis et al. [2015] found (using local probabilistic tractography) both decreased FA (bilateral

fornix, right anterior superior longitudinal fasciculus) and increased FA (thalamic radiation, left anterior longitudinal fasciculus) relative to HC. Using a local deterministic approach in a small sample of treatment-resistant adult acAN patients, Hayes et al. [2015] found decreased FA and altered AD and RD in the fornix, anterior limb of the capsula interna, cingulum and inferior front-occipital fasciculus. Together, the results describing WM microstructure in AN are inconclusive and more research is needed.

Several factors may contribute to the inconclusive results of the aforementioned studies. Some studies were based on adult patients suffering from chronic AN [Hayes et al., 2015; Kazlouski et al., 2011; Via et al., 2014] and in other studies the patients underwent a period of realimentation before scanning, and thus the patients may have been partly renourished at the time of scanning [Frank et al., 2013; Kazlouski et al., 2011; Nagahara et al., 2014; Via et al., 2014]. Furthermore, studies with smaller sample sizes are limited in their ability to control for potential confounding factors [Button et al., 2013] and previous studies included a substantial number of patients taking psychotropic medications. Furthermore, if patients and controls are not very carefully matched regarding age, developmental trajectories of WM microstructure might lead to spurious group differences [Lebel et al., 2008; Simmonds et al., 2014].

To develop a better understanding of WM microstructure in AN, the current study employed a global probabilistic tractography approach (see below) to analyze DTI data in a comparatively large and medication-free sample of both young acAN and recAN female patients relative to pairwise age-matched HC participants. The sample is largely overlapping (88% cohort acAN-HC, 94% cohort recAN-HC) with the sample in which we reported substantially reduced cortical thickness and GM volumes in the underweight state and complete normalization in recovered patients [King et al., 2015].

The DTI analysis employed in the current study is a global probabilistic tractography [Jbabdi et al., 2007] algorithm introduced by Yendiki et al. [2011]. This method, known as TRACULA—TRActs Constrained by UnderLying Anatomy—implemented in FreeSurfer [Fischl et al., 2002], provides an automated and unbiased reconstruction of the major WM pathways based on knowledge of prior distributions of the neighboring structures of each pathway derived from a set of training subjects and can effectively minimize the effects of motion artefacts known to bias DTI results [Yendiki et al., 2013]. TRACULA performs tractography in individual native space of the diffusion-weighted data and is therefore less susceptible to issues with normalization (co-registration to a common template) procedures known to be particular problematic for voxel-based methods [Jones and Cercignani, 2010]. Furthermore, in contrast to local tractography algorithms which estimate WM pathways between a seed and other connected regions in a step-by-step fashion, global tractography methods have an improved ability to isolate specific pathways by defining both tract end points and estimating all possible connections at once [Jbabdi and Johansen-Berg, 2011; Mangin et al., 2013]. As in previous studies using TRACULA, we first tested for group differences in FA, MD, RD, and AD with univariate statistics. However, given that univariate methods do not take the covariance between measures into account and may, thus, have limited ability to detect a specific combination of markers that predict membership [e.g., disease status; Schölkopf and Smola, 2002], we further scrutinized the data with a supplemental cluster analysis and a multivariate pattern classification procedure.

METHODS

Participants

The sample in the current study consisted of a total of 129 female volunteers: 35 acAN (12–24 years old) according to DSM-IV [American Psychiatric Association, 1994], 32 recAN (16–28 years old) and 62 HC (12–28 years old). The study was approved by the Institutional Review Board of the Technische Universität Dresden and all participants (or their legal guardians, if under 18 years old) gave written informed consent.

Patients with acAN were recruited from specialized eating disorder programs at a university child and adolescent psychiatry and psychosomatic medicine department and underwent magnetic resonance imaging within 96 hours after beginning behaviorally oriented nutritional rehabilitation programs.

To be considered "recovered," recAN subjects had to (1) maintain a BMI > 18.5 kg/m^2 (if older than 18 years) or a BMI >10th BMI percentile [if younger than 18 years; Kromeyer-Hauschild et al., 2001] for at least 6 months prior to the study, (2) menstruate, and (3) have not binged, purged or engaged in significant restrictive eating patterns.

HCs were recruited through advertisement among middle school, high school, and university students. To be included in the HC group, participants had to be of normal weight, eumenorrhoeic, and have no history of neurological or psychiatric illness.

Three acAN (9%) had comorbid psychiatric disorders (two depressive disorder including dysthymia and one other). In the recAN group, 22% of the participants had associated psychiatric comorbidity at the time of treatment (16% depressive disorders including dysthymia and 6% other disorders).

Information pertinent to exclusion criteria and possible confounding variables in all participants, including menstrual cycle (menstruation criteria were only applied to participants 13 years or older; see Supporting Information), eating behavior, weight history and use of contraceptive medication were obtained using the expert version of the structured interview for Anorexia and Bulimia Nervosa for DSM-IV [Fichter and Quadflieg, 2000], supplemented by our own semi-structured interview, which includes several specific questions regarding general

medical, neurological, and psychiatric history; both of which were administered by a trained master's or doctoral level interviewer. In patients, this information served as the basis for comorbid diagnoses, which were confirmed by an expert clinician with over 10 years of experience after careful chart review (including consideration of medical and psychiatric history, physical examination, routine blood tests, urine analysis and a range of additional psychiatric screening instruments). HC participants were excluded if they had any history of psychiatric illness (as assessed by the interviews described above), a lifetime BMI below the 10th BMI percentile (if younger than 18 years) or BMI below 18.5 kg/m^2 (if older than 18 years) or were currently obese (BMI over 97th BMI percentile if younger than 18 years; BMI over 30 kg/m^2 if older than 18 years). Participants of all study groups were excluded if they had a lifetime history of any of the following clinical diagnoses: organic brain syndrome, schizophrenia, substance dependence, psychosis NOS, bipolar disorder, bulimia nervosa, or binge-eating disorder (or "regular" binge eating—defined as bingeing at least once weekly for three or more consecutive months). Further exclusion criteria for all participants were IQ lower than 85, psychotropic medication within 4 weeks prior to the study, current substance abuse, current inflammatory, neurologic or metabolic illness, chronic medical or neurological illness that could affect appetite, eating behavior, or body.

Clinical Measures

To complement the information obtained with the clinical interviews, we also used the Eating Disorder Inventory (EDI-2 [Paul, 2005]), the Beck Depression Inventory (BDI-II [Hautzinger et al., 2009]), the revised Symptom Checklist 90 (SCL-90-R [Franke, 2002]) and a short version of the Wechsler Intelligence Scale for Children (HAWIK [Petermann and Daseking, 2009]) for participants aged 15 years or younger or the short version of the Wechsler Adult Intelligence Scale (WIE [von Aster et al., 2006]) for participants aged 16 years or older.

Hydration status has been shown to impact brain structure [Streitbürger et al., 2012]. As in our previous structural imaging studies in AN [King et al., 2015; Bernardoni et al., 2016], we also measured urine specific gravity to gauge hydration status in the current acAN sample. For further details regarding clinical measures, see Supporting Information.

Demographic and clinical study data were collected and managed using a secure, web-based electronic data capture tool, the Research Electronic Data Capture (REDCap [Harris et al., 2009]).

Structural Image Acquisition

T1-weighted images were acquired on the 3.0 T scanner (Magnetom Trio, Siemens, Erlangen, Germany) of the Technische Universität Dresden Neuroimaging Center using a 12 channel head coil and rapid acquisition gradient echo (MP-RAGE) sequence with the following parameters: 176 sagittal slices (1 mm thickness, no gap), TR = 1,900 ms; TE = 2.26 ms; flip angle = 9°; voxel size = 1.0 × 1.0 × 1.0 mm^3, FoV = 256 × 256 mm^2, and bandwidth of 200 Hz/pixel.

Diffusion weighted images were acquired using a spin-echo sequence with 30 diffusion directions with a diffusion weighting b of 1,300 s/mm^2 and additionally six images with b = 0. The acquisition parameters were: 2.4 mm isotropic resolution, matrix size 128 × 128, no inter slice gap, TE = 104 ms, TR = 15 s, BW = 2,056 Hz/pixel and GRAPPA acceleration factor 2. Total acquisition time was 6.1 min.

Image Analysis

Diffusion tensor analysis was performed using an automated approach with the TRACULA algorithm [version 5.3.0; Yendiki et al., 2011] within the FreeSurfer software suite (http://surfer.nmr.mgh.harvard.edu). FreeSurfer is a well-established software that also includes automated volumetric segmentation and cortical surface reconstruction of structural MR data (here T1-weighted images) into anatomically defined GM and WM regions [Dale et al., 1999; Desikan et al., 2006; Fischl and Dale, 2000; Fischl et al., 1999a,b, 2002]. TRACULA employs global probabilistic tractography with anatomical priors derived from the FreeSurfer "recon-all" procedure. Pre-processing included a correction for eddy currents employing FSL (version 5.0, http://www.fmrib.ox.ac.uk/fsl) and a least squares tensor fitting (FSL's dtifit). For global probabilistic tractography we registered the individuals' diffusion-weighted image to their FreeSurfer-segmented anatomical images and then registered it to the MNI template. For further details regarding analysis of the DTI data, see Supporting Information).

TRACULA reconstructs 18 major WM pathways: corticospinal tract (cst), uncinate fasciculus (unc), inferior longitudinal fasciculus (ilf), anterior thalamic radiations (atr), cingulum-cingulate gyrus bundle (ccg), cingulum-angular bundle (cab), superior longitudinal fasciculus-parietal terminations (slfp), superior longitudinal fasciculus-temporal terminations (slft), corpus callosum-forceps major (fmar), and corpus callosum-forceps minor (fmin). Other than the corpus callosum, pathways were reconstructed separately for each hemisphere (abbreviated as lh for left hemisphere and rh for right hemisphere). To handle possible bias due to motion artifacts, we estimated the motion measures with TRACULA 5.3.0 and calculated the total motion index (TMI) according to Yendiki et al. [2013].

Quality assurance was done for each processing step. We excluded one recAN participant due to high motion (TMI > 10). As an additional measure to limit undue influence of potentially erroneous tract reconstruction, we excluded anisotropy and diffusivity values from single tracts in single participants if the tract volume was

TABLE I. Demographic variables and clinical measures of cohort I (acAN/HC) and cohort II (recAN/HC)

	N	Sample		Analyses		
	acAN/HC recAN/HC	acAN recAN	HC_acAN HC_recAN	*t*	d*f*	*P*
Age	35/35	16.1 (2.8)	16.4 (2.6)	−0.434	68	0.666
	31/31	22.5 (3.0)	22.5 (2.9)	−0.013	60	0.990
IQ	32/34	112.5 (11.4)	110.5 (10.1)	0.527	64	0.446
	31/31	108.5 (10.0)	111.5 (8.3)	−1.274	60	0.208
BMI	35/35	14.70 (1.31)	20.75 (2.98)	−11.485	68	<0.0001
	31/31	21.09 (1.91)	21.34 (2.18)	−1.048	60	0.299
TMI	35/35	0.2257 (.23)	0.1657 (.34)	0.145	68	0.885
	31/31	0.1742 (.27)	0.2548 (.31)	−0.196	60	0.845
EDI-2 (drive for thinness)	35/35	26.11 (10.30)	13.89 (6.86)	5.846	68	<0.0001
	31/31	18.97 (10.74)	12.97 (4.96)	2.825	60	0.006
BDI-II	35/35	20.49 (11.91)	5.55 (5.71)	6.686	68	<0.0001
	31/31	8.35 (8.37)	4.67 (6.22)	1.966	60	0.054

Acutely underweight anorexia nervosa patients (acAN) were age-matched with healthy controls (HC_acAN), and recovered patients (recAN) were age-matched with healthy controls (HC_recAN). All values are means and standard deviation except for TMI (standard error of the mean). The average duration since weight normalization in the recAN group was 57.0 ± 33 (SD) months (range: 6–140 months). The duration of recovery in 2 recAN was <12 months. Abbreviations: d*f*, degrees of freedom; BMI, body mass index (test statistics are based on BMI Standard Deviation Score, see Supporting Information); IQ, intelligence quotient; TMI, total motion index; EDI-2, Eating Disorder Inventory; BDI-II, Beck Depression Inventory-II.

excessively small or large (±3 SD) relative to the rest of the diagnostic group. Using this criterion, 35 outliers (1.5%) in 25 participants (6 acAN, 7 recAN, 12 HC) were identified (see also Supporting Information).

Finally, we obtained mean values of FA, MD, RD, and AD as well as tract volume in each of the 18 WM pathways and for each participant.

Statistical Analyses

Given the age difference between the acAN and recAN groups (the acAN was predominately adolescent, while the recAN group was primarily young adult; see Table I), two independent group comparisons of the DTI data were performed: (1) acAN versus HC and (2) recAN versus HC. To ensure appropriate comparisons, we carried out case-control age-matching using an automated search algorithm for optimal pairs [propensity score; Leuven and Sianesi, 2003]. The maximum age difference between the individuals within one pair was 2 years for both the acAN-HC and the recAN-HC group (acAN-HC mean age difference within a matched pair was 0.8 years, recAN-HC mean age difference within a matched pair was 0.6 years). Four HCs were in both groups, that is, the matching algorithm assigned them for comparison with acAN and recAN. Mean age and variance for patients and HC was similar in both groups (Table I).

Following Yendiki et al. [2011, 2013], we used analysis of covariance for each of the four DTI parameters (FA, MD, RD, AD) as well as tract volume with group as predictor and both age and TMI as nuisance regressors (Tables II and III). Using the same basic regression model, we explored whether depressive symptoms (BDI-II scores) or IQ might explain group differences in the four DTI measures. For the analysis of covariance with IQ as predictor, we replaced missing values (3 acAN, 1 HC) with the respective group mean score. Additional regression models explored whether "drive for thinness" (EDI-2 subscale scores) and depressive symptoms (BDI-II scores) covaried with WM microstructure parameters in any tracts within either the acAN or recAN sample.

To control for multiple testing, the level of statistical significance for each tract was corrected using a False Discovery Rate [FDR; Benjamini and Hochberg, 1995] of $q < 0.05$ across all four WM metrics and across all tracts simultaneously. For exploratory analysis, we used a more liberal approach—uncorrected *P*-values with a threshold of 0.01. Since univariate methods do not account for potentially meaningful relationships between combinations of measures in which the groups might differ, we also performed a k-means clustering analysis as well as an analysis using a machine learning algorithm to test whether a combination of the DTI metrics can help to predict group membership (Supporting Information).

Analysis of standard WM volume data (obtained using a standard "recon-all" FreeSurfer analysis of T1-weighted MRI data) is described in Supporting Information.

If not indicated otherwise, all values are presented as mean ± SD. All tests were performed with SPSS statistical software version 21.0 (SPSS, Chicago, Illinois).

RESULTS

Demographic and Clinical Characteristics

The demographic and clinical characteristics of the acAN, recAN, and respective HC groups are summarized

TABLE II. Comparison of DTI parameters between acAN and HC

	FA					MD					RD					AD				
Tract	df	F_{group}	P_{group}	$\eta 2$	FDR	df	F_{group}	pgroup	$\eta 2$	FDR	df	F_{group}	P_{group}	$\eta 2$	FDR	df	F_{group}	P_{group}	$\eta 2$	FDR
fmajor	1.69	1.78	0.185	0.026	0.403	1.69	2.92	0.092	0.042	0.414	1.69	0.094	0.760	0.001	0.855	1.69	0.000	1.00	0.000	1.00
fminor	1.69	1.50	0.224	0.022	0.403	1.69	1.86	0.178	0.027	0.522	1.69	2.32	0.132	0.034	0.380	1.69	0.111	0.740	0.002	.888
lh atr	1.69	0.884	0.350	0.013	0.522	1.69	0.152	0.698	0.002	0.821	1.69	0.451	0.504	0.007	0.663	1.69	0.066	0.799	0.001	.898
lh cab	1.65	6.82	0.011	0.099	0.198	1.65	0.065	0.800	0.001	0.847	1.65	1.49	0.226	0.024	0.421	1.65	3.13	0.082	0.048	.306
lh ccg	1.68	0.701	0.406	0.011	0.522	1.68	1.29	0.259	0.020	0.522	1.68	0.013	0.909	0.001	0.962	1.68	4.73	0.033	0.070	.198
lh cst	1.69	2.65	0.108	0.039	0.324	1.69	4.96	0.029	0.070	0.174	1.69	4.16	0.045	0.059	0.380	1.69	2.20	0.143	0.032	.342
lh ilf	1.69	4.30	0.042	0.061	0.294	1.69	0.020	0.887	0.000	0.887	1.69	3.03	0.086	0.044	0.380	1.69	2.74	0.102	0.040	.306
lh slfp	1.69	4.00	0.049	0.057	0.294	1.69	0.120	0.730	0.002	0.821	1.69	0.323	0.572	0.005	0.686	1.69	2.75	0.102	0.040	.306
lh slft	1.69	0.738	0.393	0.110	0.522	1.69	1.40	0.240	0.021	0.522	1.69	1.93	0.169	0.028	0.380	1.69	0.128	0.721	0.002	.888
lh unc	1.69	0.046	0.830	0.001	0.879	1.69	0.953	0.333	0.014	0.545	1.69	0.571	0.452	0.009	0.663	1.69	0.453	0.503	0.007	.696
rh atr	1.67	2.33	0.132	0.035	0.339	1.67	0.136	0.713	0.002	0.821	1.67	1.20	0.277	0.018	0.453	1.67	1.20	0.277	0.018	.498
rh cab	1.68	3.33	0.072	0.049	0.324	1.68	1.28	0.261	0.019	0.522	1.68	2.13	0.149	0.032	0.380	1.68	0.006	0.940	0.000	.995
rh ccg	1.68	0.141	0.708	0.002	0.849	1.68	0.711	0.402	0.011	0.603	1.68	0.427	0.516	0.007	0.663	1.68	0.507	0.479	0.008	.696
rh cst	1.68	1.57	0.215	0.024	0.403	1.68	5.99	0.017	0.084	0.153	1.68	3.56	0.064	0.052	0.380	1.68	2.09	0.152	0.031	.342
rh ilf	1.69	1.20	0.275	0.018	0.450	1.69	0.205	0.652	0.003	0.821	1.69	1.99	0.162	0.029	0.380	1.69	0.706	0.404	0.011	.661
rh slfp	1.69	2.77	0.100	0.040	0.324	1.69	0.968	0.329	0.014	0.545	1.69	0.001	1.00	0.000	1.00	1.69	5.51	0.022	0.077	.198
rh slft	1.68	0.001	0.986	0.000	0.986	1.68	6.29	0.015	0.088	0.153	1.68	2.52	0.117	0.037	0.380	1.68	8.23	**0.006**	0.112	.108
rh unc	1.66	0.065	0.800	0.001	0.879	1.66	2.49	0.119	0.038	0.428	1.66	1.44	0.234	0.022	0.421	1.66	1.57	0.214	0.024	.428

Note that age and TMI were covariates. Their corresponding F and P values can be found in Supporting Information Table S5. Bold: significant at $P < 0.01$ (uncorrected). Abbreviations: Fmajor, corpus callosum–forceps major; fminor, corpus callosum–forceps minor; lh, left hemispheric; rh, right hemispheric; atr, anterior-thalamic radiations; cab, cingulum–angular bundle; ccg, cingulum–cingulate gyrus bundle; cst, corticospinal tract; ilf, inferior longitudinal fasciculus; slfp, superior longitudinal fasciculus-parietal terminations; slft, superior longitudinal fasciculus – temporal terminations; unc, uncinate fasciculus; FA, fractional anisotropy; MD, mean diffusivity; RD, radial diffusivity; AD, axial diffusivity; $\eta 2$, effect size; FDR, false discovery rate. For all other abbreviations please refer to legend of Table I.

TABLE III. Comparison of DTI parameters between recAN and HC

	FA					MD					RD					AD				
Tract	d*f*	F_{group}	P_{group}	$\eta 2$	FDR	d*f*	F_{group}	P_{group}	$\eta 2$	FDR	d*f*	F_{group}	P_{group}	$\eta 2$	FDR	*df*	F_{group}	P_{group}	$\eta 2$	FDR
fmajor	1.61	1.27	0.637	0.021	0.819	1.61	0.694	0.408	0.012	0.432	1.61	0.965	0.330	0.016	0.495	1.61	0.000	1.00	0.000	1.00
fminor	1.61	2.25	0.139	0.037	0.313	1.61	5.18	0.027	0.082	0.122	1.61	0.965	0.330	0.016	0.495	1.61	0.688	0.410	0.012	0.644
lh atr	1.59	3.75	0.058	0.063	0.313	1.59	4.17	0.046	0.070	0.166	1.59	6.68	0.012	0.106	0.072	1.59	0.021	0.884	0.001	1.00
lh cab	1.59	0.874	0.354	0.015	0.490	1.59	2.80	0.100	0.048	0.238	1.59	2.38	0.128	0.041	0.329	1.59	0.911	0.344	0.016	0.644
lh ccg	1.59	0.026	0.873	0.001	0.913	1.59	0.435	0.512	0.008	0.512	1.59	0.103	0.750	0.002	0.794	1.59	0.708	0.404	0.012	0.644
lh cst	1.59	4.19	0.045	0.070	0.313	1.59	6.72	0.012	0.107	0.102	1.59	7.32	**0.009**	0.116	0.072	1.59	2.83	0.098	0.048	0.336
lh ilf	1.61	2.73	0.104	0.045	0.313	1.61	1.79	0.186	0.030	0.304	1.61	4.02	0.050	0.065	0.150	1.61	0.085	0.771	0.001	0.991
lh slfp	1.60	1.36	0.248	0.023	0.450	1.60	2.51	0.119	0.042	0.238	1.60	0.261	0.612	0.005	0.787	1.60	7.79	**0.007**	0.120	0.126
lh slft	1.61	1.21	0.275	0.021	0.490	1.61	5.99	0.017	0.094	0.102	1.61	4.34	0.042	0.07	0.150	1.61	4.07	0.048	0.066	0.297
lh unc	1.59	0.067	0.797	0.001	0.899	1.59	1.06	0.307	0.019	0.432	1.59	0.667	0.418	0.012	0.579	1.59	1.41	0.240	0.025	0.540
rh atr	1.60	3.15	0.081	0.052	0.313	1.60	6.08	0.017	0.096	0.102	1.60	7.19	**0.010**	0.112	0.072	1.60	0.635	0.429	0.011	0.644
rh cab	1.61	2.61	0.112	0.043	0.313	1.61	0.882	0.352	0.015	0.432	1.61	1.63	0.207	0.027	0.414	1.61	0.001	1.00	0.000	1.00
rh ccg	1.60	1.02	0.318	0.018	0.477	1.60	0.782	0.380	0.014	0.432	1.61	<0.001	1.00	0.000	1.00	1.60	2.61	0.112	0.044	0.336
rh cst	1.60	1.21	0.275	0.021	0.450	1.60	1.90	0.173	0.032	0.304	1.60	2.09	0.154	0.035	0.347	1.60	0.156	0.695	0.003	0.962
rh ilf	1.61	3.26	0.076	0.053	0.312	1.61	2.66	0.108	0.044	0.238	1.61	5.35	0.024	0.084	0.108	1.61	0.001	1.00	0.000	1.00
rh slfp	1.60	2.41	0.126	0.041	0.312	1.60	0.694	0.408	0.012	0.432	1.60	0.143	0.706	0.003	0.794	1.60	3.50	0.066	0.058	0.297
rh slft	1.60	0.012	0.913	0.001	0.913	1.60	0.885	0.351	0.015	0.432	1.60	0.19	0.665	0.003	0.794	1.60	1.67	0.202	0.028	0.519
rh unc	1.60	0.065	0.799	0.001	0.899	1.60	2.94	0.092	0.049	0.238	1.60	1.21	0.276	0.021	0.495	1.60	3.81	0.056	0.063	0.297

Note that age and TMI were covariates. Their corresponding F and P values can be found in Supporting Information Table S6. Bold: significant at $P < 0.01$ (uncorrected). For abbreviations please refer to Tables I and II.

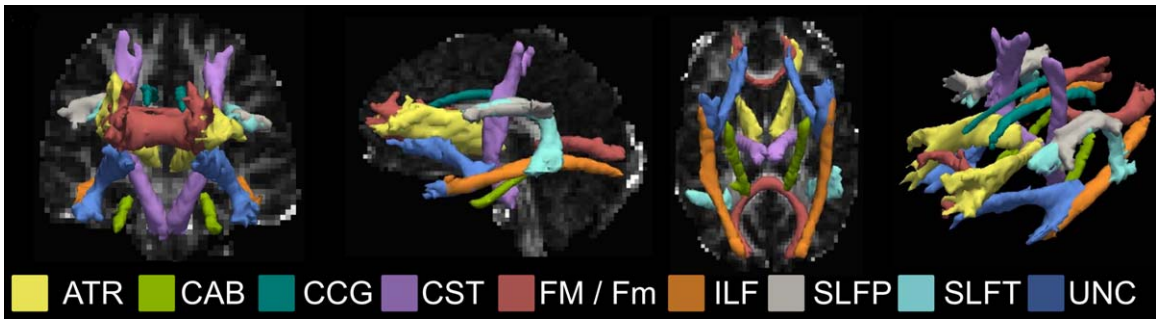

Figure 1.

Visualization of white matter tracts as reconstructed by TRACULA (displayed at 20% of their maximum threshold) are overlaid on selected slices of fractional anisotropy maps (from left to right, coronal, sagittal, axial) and a 3D anatomical view (far right) of a representative HC patient whose age and BMI approximated the group mean (age = 16.1 years, BMI = 20.1). ATR, anterior thalamic radiation; CAB, cingulum-angular bundle; CCG, cingulum-cingulate gyrus bundle; CST, corticospinal tract; FM, corpus callosum-forceps major; Fm, corpus callosum-forceps minor; ILF, inferior longitudinal fasciculus; SLFP, superior longitudinal fasciculus-parietal ending; SLFT, superior longitudinal fasciculus-temporal ending; UNC, unicate fasciculus.

in Table I. Neither acAN nor recAN differed in age, motion during scanning (TMI), or IQ relative to their HC counterparts. As expected, (age-adjusted) BMI was significantly lower in the acAN group relative to the corresponding HCs, but did not differ from that of the matched HCs for recAN. RecAN still showed some residual eating disorder symptoms, but depressive symptoms were not significantly different between recAN and HC.

Group Comparisons: acAN-HC

Figure 1 presents the reconstructed tracts for one representative HC participant. There were no statistically significant differences (FDR) in WM tract volumes or overall cortical-, cerebellar-, or corpus callosum WM volumes when comparing acAN and HC (Supporting Information, Tables S1 and S3). There were also no differences (FDR) in FA, MD, RD, and AD between the groups in any of the tracts. At a considerably less conservative statistical threshold ($p < 0.01$, uncorrected), AD was lower in acAN in rh slft (Fig. 2, Table II; see also Supporting Information Table S5). Including depressive symptoms (BDI-II scores) or IQ as a covariate did not change these results (FDR, see Supporting Information Tables S7 and S11). The results were also not changed by limiting the analysis to adolescent participants under 18 years old (Supporting Information Table S16). Supplementary cluster analysis based on all tracts and DTI metrics yielded no significant difference in the number of acAN and HC in the two clusters (Supporting Information Table S13), that is, no clinically meaningful partitioning. However, a machine learning algorithm did show some predictive ability to separate acAN from HC (Supporting Information Fig. S1). Nonetheless, the results were not clearly in line with a hypothesis of impaired WM integrity in the patients (Supporting Information, Table S15).

Group Comparisons: recAN-HC

Neither WM tract volumes, nor overall cortical-, cerebellar-, or corpus callosum WM volumes differed significantly (FDR) between recAN and HC (Supporting Information Tables S2 and S4). There were also no statistically significant differences (FDR) in FA, MD, RD, and AD between recAN and HC in any of the tracts either in the entire sample (Fig. 3, Table III; see also Supporting Information Table S6) or a sub-sample including only adults over the age of 18 years (Supporting Information Table S17). In exploratory analysis using lenient uncorrected *P*-values ($P < 0.01$), the following group differences were evident: reduced RD in lh cst and rh atr and reduced AD in lh slfp for recAN compared with HC (Fig. 3, Table III, see also Supporting Information Table S6). Including depressive symptoms (BDI-II scores) as a covariate did not have any significant effect (FDR) on these results (Supporting Information Table S8), but analysis of covariance with IQ did reveal reduced RD in the lh and rh atr in recAN compared with HC (FDR; Supporting Information Table S12). Supplementary cluster analysis yielded no clinically meaningful partitioning (Supporting Information Table S13) and a machine learning algorithm did not help to predict group membership (Supporting Information Fig. S1).

Associations with Clinical Characteristics Within acAN AND recAN

In order to explore whether drive for thinness (EDI-2) and depression (BDI-II) scores were associated with indices of WM integrity within either the acAN or recAN groups, we added these scores as covariates in a regression model. In acAN, after correcting for multiple comparisons using FDR ($q < 0.05$) none of the tracts were associated with either drive for thinness or depressive

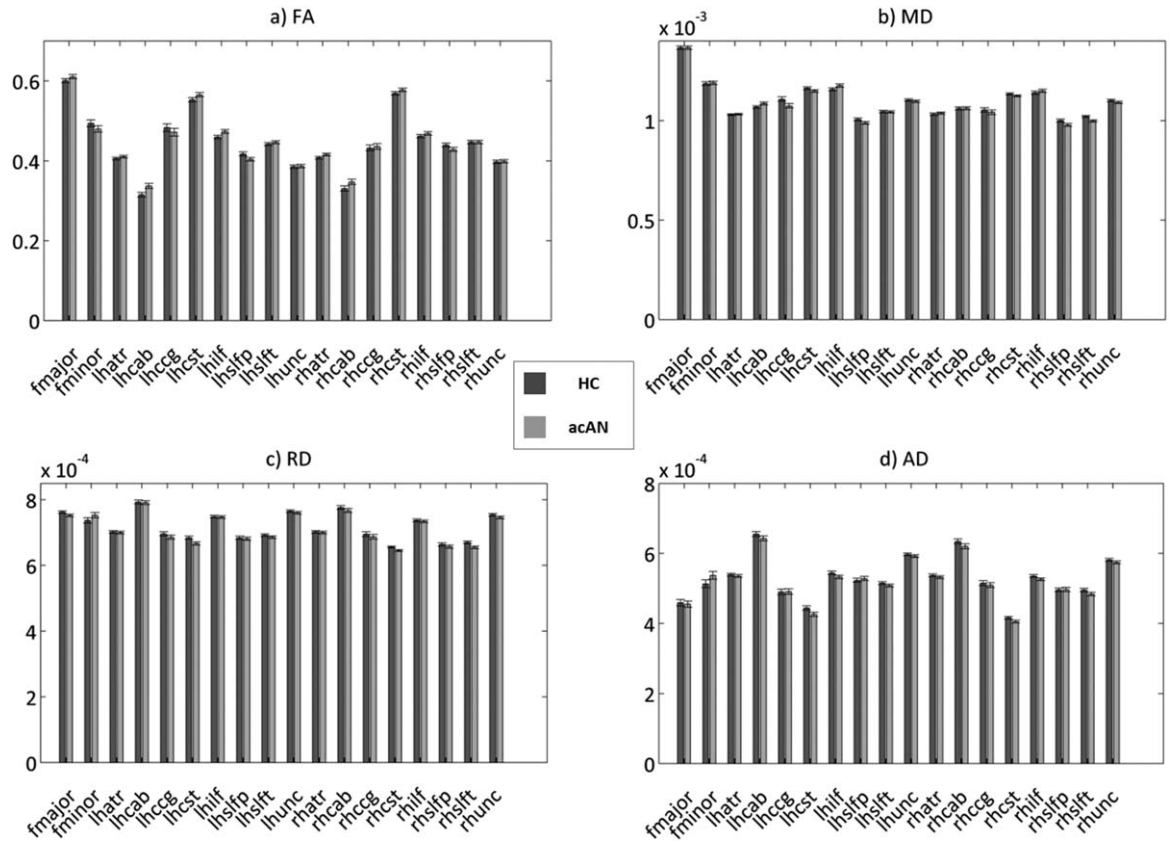

Figure 2.

acAN-HC comparison. Mean FA, MD, RD, and AD for each of the 18 pathways reconstructed by TRACULA are plotted for the acAN and age-matched HC group. Group averages and standard error bars are shown.

symptoms (Supporting Information Table S9). In recAN, a positive association between drive for thinness and FA in the rh atr was revealed, but no association with depression was evident (Supporting Information Table S10).

Measurements of hydration status in acAN patients were in the normal range (Supporting Information). Therefore, we did not conduct further testing for correlations with measures of anisotropy or diffusivity.

DISCUSSION

In this study we evaluated WM microstructure in one of the largest samples of young patients with both acAN and recAN. Controlling for motion and applying strict measures to exclude possible bias due to age, early realimentation, circadian fluctuations or medication, we did not find any significant volumetric differences or microstructural abnormalities in 18 WM tracts in young acAN nor recAN compared with pair-wise age-matched HC. Supporting and extending these findings, cluster analyses applied to all WM microstructure metrics simultaneously did not reveal any patterns that would predict group membership. However, a machine learning algorithm showed some potential to differentiate acAN from HC, but not recAN from HC.

The volumes of the WM tracts (based on tractography results) as well as total cortical WM volume, cerebellar and corpus callosum WM volumes (assessed with the standard FreeSurfer technique based on T1-weighted images) were similar to age-matched HC. Similarly, previous studies also found no group differences in WM volume [Frank et al., 2013; Kazlouski et al., 2011; Via et al., 2014] or even increased WM volume in temporal lobe areas in acAN [Frank et al., 2013]. Seitz et al. [2014] reviewed GM and WM changes in AN. In contrast to robust group differences in GM volume, only seven out of 13 studies reported significant WM volume reduction in acAN, while WM reductions in recAN were generally not significant.

Our findings of relatively intact WM microstructure stand in contrast to most previous DTI studies both in acAN [Frank et al., 2013; Frieling et al., 2012; Hayes et al., 2015; Kazlouski et al., 2011; Nagahara et al., 2014; Travis

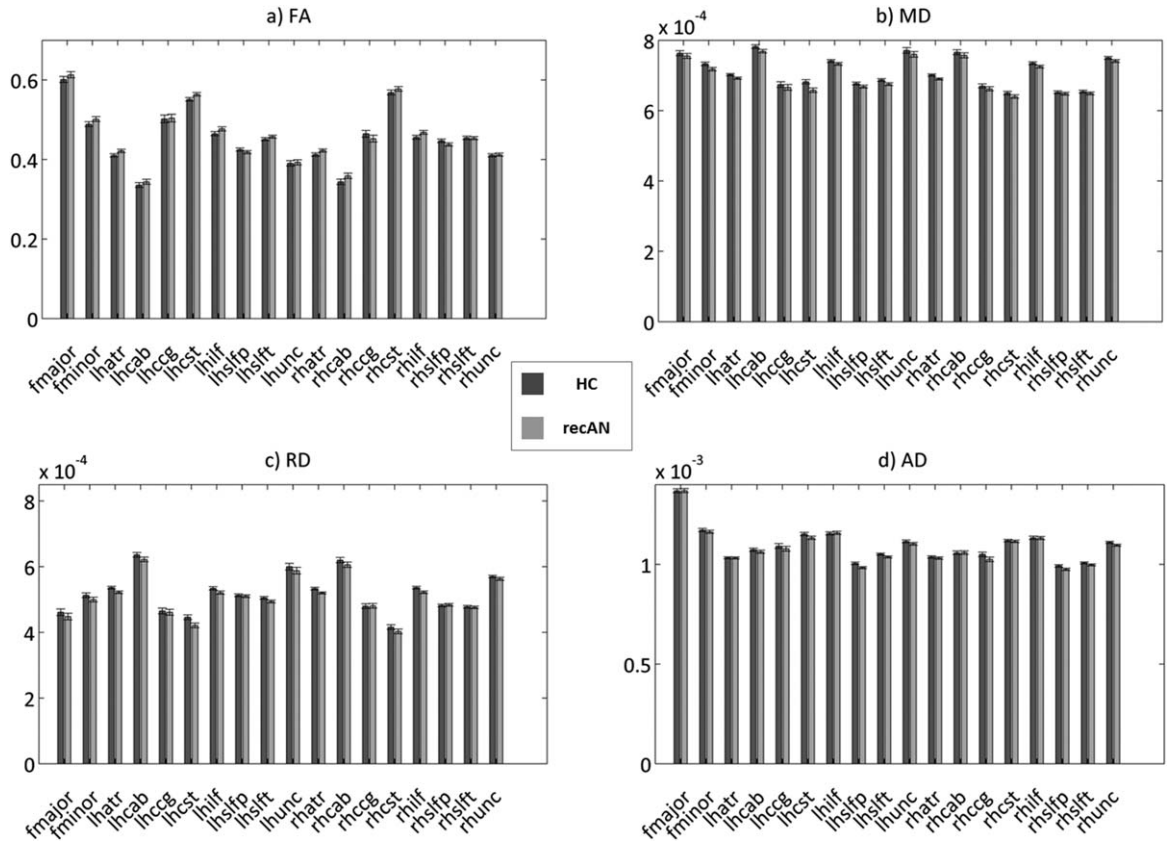

Figure 3.
recAN-HC comparison. Mean FA, MD, RD, and AD for each of the 18 pathways reconstructed by TRACULA are plotted for the recAN and age-matched HC group. Group averages and standard error bars are shown.

et al., 2015; Via et al., 2014; Vogel et al., 2016] and recAN [Yau et al., 2013; Shott et al., 2015] which have shown some evidence of altered WM microstructure in the disorder. For example, one of the largest ($n = 19$) studies in acAN to date [Via et al., 2014] found significantly reduced FA in patients (age range: 18–49) in the slf and increased MD in the fornix using tract-based spatial statistics (TBSS; a voxelwise technique in which participants' FA is projected onto a common WM skeleton by filling each skeleton voxel with the maximum FA value found along the perpendicular tract direction). However, in line with our and others' findings [Frank et al., 2013; Nagahara et al., 2014; Vogel et al., 2016], this study did not find any correlations between measures of WM microstructure and eating disorder symptoms (other than BMI) or harm avoidance [but see Kazlouski et al., 2011]. We also explored the potential influence of depressive symptoms both within the patient groups and relative to HC; finding that intact WM microstructure in AN was not mediated by elevated levels of depression. Another example comes from the most recent investigation of WM microstructure in a comparably large sample of adolescent acAN ($n = 22$) which found FA to be increased in patients in widespread bilateral areas of frontal, parietal and temporal cortex. When considered in relation to previous findings in adult samples, these findings in a typical adolescent sample suggest that alterations in WM microstructure in AN may reflect a highly time-dependent pathomechanism that can vary dynamically as a function of chronicity.

The first study to focus on recAN [Yau et al., 2013] found no differences in FA in a small sample ($n = 12$), but lower MD in the posterior cingulum, precuneus, SLF, corpus callosum, capsula interna and corona radiata in recAN compared with HC; suggestive of preserved (or recovered) WM integrity (at least in patients with less severe illness history). This is generally compatible with the suggestive evidence for reduced RD in recAN found here in a supplementary analysis exploring possible effects of IQ in bilateral atr (Supporting Information Table S12). In contrast, Frieling et al. [2012] reported reduced FA in the thalamic radiation, but this finding was based on a mixed sample of acAN and recAN. Last but not least, the recent study in recAN [Shott et al., 2015] using fiber-tracking between selected reward-related ROIs found a combination of

increased connectivity and decreased FA, which was interpreted to reflect WM remodeling after impairments during the underweight state. Considered in relation to these divergent previous findings in both acAN and recAN, the current results including the discriminative ability of the applied machine learning algorithm (Supporting Information Fig. S1; Table S15) are not clearly in line with a straightforward hypothesis such as "impaired WM microstructure in acAN," but seem to point more toward a complex pattern of either subtle increases or decreases in anisotropy and diffusivity in AN depending on a range of variables including age, age of illness onset, duration, and severity of illness, intellectual functioning, nutritional state, or specific WM pathway.

In addition to excluding patients taking psychotropic medication, we took several extra measures to control for potentially confounding factors that might have affected the results of previous DTI studies in AN (and hence may explain the previous heterogeneous evidence). First, no known studies have corrected for head motion beyond the simple algorithm that is part of eddy current correction. A recent article demonstrated that group differences in DTI metrics can emerge simply due to the fact that some patient populations show more head motion during scanning than the HC [Yendiki et al., 2013]. Second, it has been suggested that WM integrity correlates positively with IQ, especially in frontal and occipito-parietal areas [Schmithorst et al., 2005]. IQ has been reported to be above average in AN [Lopez et al., 2010]—a circumstance which could potentially have explained our findings. However, in our samples there were no group differences in IQ and the inclusion of IQ into our models did not change our results in acAN (and revealed reduced RD in recAN). Of note, IQ in acAN was not measured in the acutely underweight state in the current sample. Thus, it is unlikely that IQ was underestimated. Third, many studies have scanned acAN patients more than a week after starting realimentation [Frank et al., 2013; Kazlouski et al., 2011; Via et al., 2014] or did not clearly specify this important variable [Frieling et al., 2012; Nagahara et al., 2014; Travis et al., 2015]. As recently discussed in an expert commentary by Frank [2015b], variance in time between start of realimentation and scanning might account for differences between structural MRI studies in AN.

Although all DTI analysis methods have their own set of advantages and disadvantages [Jones et al., 2013], tractography [Parker et al., 2002; Schmahmann et al., 2007] and more specifically, global tractography [Mangin et al., 2013; Jbabdi and Johansen-Berg, 2011] as used in our study, is considered one of the most accurate methods for identifying WM tracts and their characteristics. An automatic tract identification method as implemented in TRACULA, overcomes many of the disadvantages of previous tractography methods, which were relying on ROIs [Yeatman et al., 2012; Yendiki et al., 2011]. In contrast, voxelwise measures suffer from insufficient precision to align brain images of subjects to a common coordinate frame. Accordingly, the analysis is sensitive to variations in tract size and shape. The TBSS approach employed in several recent studies in AN (see "Introduction" section) can also not ensure that voxels correspond to the same tract across subjects [Yeatman et al., 2012] and is based on the assumption that microstructural abnormalities are spatially homogeneous [White et al., 2009]. Further, Maximov et al. [2015] have shown that the results obtained with TBSS depend on the fitting algorithm, reducing reproducibility among labs.

Another reason for the heterogeneity of previous findings might lie within the high inter-subject variability of DTI metrics. Variability is highest for the mean tract volume, followed by FA and lowest for MD [Heiervang et al., 2006; Szczepankiewicz et al., 2013; see also Supporting Information Table S14). Accordingly, given the relatively small sample sizes in most previous studies, it may be possible to detect meaningful and valid group differences in MD, but rarely in FA. Furthermore, differences between studies in scanner field strength, voxel sizes, angular resolution, and patient characteristics might also explain some of the heterogeneity.

Given massively reduced cortical thickness and GM volumes in acAN (which are comparable to findings in Alzheimer's patients [King et al., 2015])—our findings of preserved WM microstructure are somewhat surprising. It may explain, why (adolescent) acAN patients often do not show marked impairments in executive functioning [Lang et al., 2014; Muetzel et al., 2015; Sarrar et al., 2011]. Possibly, relatively intact WM structures may provide the basis of the reported reversibility of GM atrophy in AN and illness recovery in general [King et al., 2015; Bernardoni et al., 2016]. In fact, our results may shed some light onto the pathophysiology of GM atrophy in AN. The lack of significant WM changes in acAN may indicate that neurons and their axons remain intact and GM volume reductions can be attributed to changes in neuronal size and dendritic remodeling [Diaz-Cintra et al., 1994; Lerch et al., 2011]. In contrast, a study in patients with bulimia nervosa found that reduced cortical volume was driven by underlying white matter changes [Marsh et al., 2015; see also Frank, 2015c]. Preserved WM integrity, does not mean that brain connectivity is completely unaffected in acAN and recAN. In fact, we and others have recently shown that functional resting state connectivity in young acAN is different from HC. We found increased path length and assortativity on a global level [Geisler et al., 2015] and reduced connectivity of the insula (and associated subcortical regions) on an intermediate and regional level [Boehm et al., 2014; Ehrlich et al., 2015; Geisler et al., 2015]. Furthermore, connectivity within the frontoparietal (cognitive control) network and in the somatosensory network has been shown to be increased in acAN [Boehm et al., 2014; Favaro et al., 2012; Lee et al., 2014]. More rigorous functional resting state connectivity studies especially in recAN

are needed to understand the reversibility of these phenomena.

Our study has to be considered in the light of the following limitations: First, we recruited mainly adolescents with first-episode AN and recAN which often have not suffered from long and chronic AN. One potential source for discrepancies between the current work and previous studies may thus be the varying duration of illness and recovery—therefore, our results may not generalize to all patients with AN. Second, undernutrition can lead to delayed maturation of endocrine systems as well as brain systems which may bias matching procedures that rely on chronological age [Lacey et al., 1979; Pozo and Argente, 2002]. However, such developmental differences should theoretically lead to even more pronounced differences in WM characteristics. Third, current DTI techniques may miss subtle or more focal WM changes that may be detectable with higher angular or spatial resolution. Indeed, a limitation of the employed global probabilistic tractography approach as implemented here in TRACULA is that DTI metrics are averaged over relatively large fiber paths and, thus, may not capture more localized changes in WM integrity. Furthermore, while univariate statistics were unable to detect any noteworthy statistical differences between the groups, multivariate pattern classification techniques applied to all DTI metrics simultaneously had showed some discriminant ability to separate acAN from HC (but not recAN from HC). Whether the benefits of studying adolescent acAN at 7 Tesla outweigh potential side effects and discomfort is still a matter of debate. Finally, the current results are not directly comparable to those that might be obtained with other DTI processing algorithms such as TBSS or local tractography and future studies are needed to compare the different approaches.

CONCLUSION

In conclusion, in a well-powered sample of young acAN as well as recAN patients, we found preserved WM tract volumes and integrity in comparison to age-matched HC, while controlling for a range of possible confounders. This finding stands in contrast to massively reduced (but largely reversible) GM volume and cortical thickness in a largely overlapping sample [King et al., 2015; Bernardoni et al., 2016], but may help to explain the relatively preserved cognitive performance of AN patients [Fowler et al., 2006; Lopez et al., 2010; Sarrar et al., 2011]. Although our finding needs replication, it is encouraging for patients, parents and therapists alike since it suggests that the structural brain connectome is not severely affected by acute (non-chronic) undernutrition and may provide an explanation for the recovery of other brain functions during weight-restoration.

CONFLICTS OF INTEREST

In the last two years, Dr. Roessner has received lecture fees from Eli Lilly, Janssen-Cilag, Medice, Novartis and was a member of advisory boards of Eli Lilly, Novartis. All other authors declare that there are no conflicts of interest in relation to the subject of this study.

ACKNOWLEDGMENTS

The authors would like to express their gratitude to J. Petermann, F. Neidel, L. Flohr, L. Scheuvens and C. Nicklisch for their assistance with participant recruitment and data collection.

REFERENCES

American Psychiatric Association. (1994). Diagnostic and Statistical Manual of Mental Disorders: DSM-IV, 4th ed. Washington, DC: American Psychiatric Association.

American Psychiatric Association (2000). Diagnostic and Statistical Manual of Mental Disorders, 4th ed., Text Revision. Washington, DC: American Psychiatric Association.

Alexander AL, Lee JE, Lazar M, Field AS (2007): Diffusion tensor imaging of the brain. Neurotherapeutics 4:316–329.

Benjamini Y, Hochberg Y (1995): Controlling the false discovery rate - a practical and powerful approach to multiple testing. J R Stat Soc Ser B-Method 57:289–300.

Bernardoni F, King JA, Geisler D, Stein E, Jaite C, Nätsch D, Tam FI, Boehm I, Seidel M, Roessner V, Ehrlich S (2016): Weight restoration therapy rapidly reverses cortical thinning in anorexia nervosa: A longitudinal study. Neuroimage 130: 214–222.

Boehm I, Geisler D, King JA, Ritschel F, Seidel M, Deza Araujo Y, Petermann J, Lohmeier H, Weiss J, Walter M, Roessner V, Ehrlich S (2014): Increased resting state functional connectivity in the fronto-parietal and default mode network in anorexia nervosa. Front Behav Neurosci 8:346.

Boghi A, Sterpone S, Sales S, D'Agata F, Bradac GB, Zullo G, Munno D (2011): In vivo evidence of global and focal brain alterations in anorexia nervosa. Psychiatry Res 192:154–159.

Button KS, Ioannidis JPA, Mokrysz C, Nosek BA, Flint J, Robinson ESJ, Munafò MR (2013): Power failure: Why small sample size undermines the reliability of neuroscience. Nat Rev Neurosci 14:365–376.

Dale AM, Fischl B, Sereno MI (1999): Cortical surface-based analysis - I. Segmentation and surface reconstruction. Neuroimage 9:179–194.

Desikan RS, Segonne F, Fischl B, Quinn BT, Dickerson BC, Blacker D, Buckner RL, Dale AM, Maguire RP, Hyman BT, Albert MS, Killiany RJ (2006): An automated labeling system for subdividing the human cerebral cortex on MRI scans into gyral based regions of interest. Neuroimage 31:968–980.

Diaz-Cintra S, Garcia-Ruiz M, Corkidi G, Cintra L (1994): Effects of prenatal malnutrition and postnatal nutritional rehabilitation on CA3 hippocampal pyramidal cells in rats of four ages. Brain Res 662:117–126.

Ehrlich S, Lord AR, Geisler D, Borchardt V, Boehm I, Seidel M, Ritschel F, Schulze A, King JA, Weidner K, Roessner V, Walter M (2015): Reduced functional connectivity in the thalamo-

insular subnetwork in patients with acute anorexia nervosa. Hum Brain Mapp 36:1772–1781.

Favaro A, Santonastaso P, Manara R, Bosello R, Bommarito G, Tenconi E, Di Salle F (2012): Disruption of visuospatial and somatosensory functional connectivity in anorexia nervosa. Biol Psychiatry 72:864–870.

Fichter M, Quadflieg N (2000): Structured interview for anorectic and bulemic eating disorders. Questionnaire and interview according to DSM-IV and ICD-10. Z Klin Psychol Psych 29: 142–143.

Fischl B, Dale AM (2000): Measuring the thickness of the human cerebral cortex from magnetic resonance images. Proc Natl Acad Sci U S A 97:11050–11055.

Fischl B, Sereno MI, Dale AM (1999a): Cortical surface-based analysis - II: Inflation, flattening, and a surface-based coordinate system. Neuroimage 9:195–207.

Fischl B, Sereno MI, Tootell RBH, Dale AM (1999b): High-resolution intersubject averaging and a coordinate system for the cortical surface. Human Brain Mapp 8:272–284.

Fischl B, Salat DH, Busa E, Albert M, Dieterich M, Haselgrove C, van der Kouwe A, Killiany R, Kennedy D, Klaveness S, Montillo A, Makris N, Rosen B, Dale AM (2002): Whole brain segmentation: Automated labeling of neuroanatomical structures in the human brain. Neuron 33:341–355.

Fowler L, Blackwell A, Jaffa A, Palmer R, Robbins TW, Sahakian BJ, Dowson JH (2006): Profile of neurocognitive impairments associated with female in-patients with anorexia nervosa. Psychol Med 36:517–527.

Frank GK (2015a): Recent advances in neuroimaging to model eating disorder neurobiology. Curr Psychiatry Rep 17:559.

Frank GK (2015b): Advances from neuroimaging studies in eating disorders. CNS Spectr 20:391–400.

Frank GK (2015c): What causes eating disorders, and what do they cause? Biol Psychiatry 77:602–603.

Frank GK, Shott ME, Hagman JO, Yang TT (2013): Localized brain volume and white matter integrity alterations in adolescent anorexia nervosa. J Am Acad Child Adolesc Psychiatry 52: 1066–1075 e5.

Franke G. (2002): SCL-90-R. Symptom-Checkliste von L. R. Derogatis-Deutsche Version. Göttingen: Beltz Test GMBH.

Frieling H, Fischer J, Wilhelm J, Engelhorn T, Bleich S, Hillemacher T, Dorfler A, Kornhuber J, de Zwaan M, Peschel T (2012): Microstructural abnormalities of the posterior thalamic radiation and the mediodorsal thalamic nuclei in females with anorexia nervosa–a voxel based diffusion tensor imaging (DTI) study. J Psychiatr Res 46:1237–1242.

Geisler D, Borchardt V, Lord AR, Boehm I, Ritschel F, Zwipp J, Clas S, King JA, Wolff-Stephan S, Roessner V, Walter M, Ehrlich S (2015): Abnormal functional global and local brain connectivity in female patients with anorexia nervosa. J Psychiatry Neurosci 40:140310.

Harris PA, Taylor R, Thielke R, Payne J, Gonzalez N, Conde JG (2009): Research electronic data capture (REDCap)–a metadata-driven methodology and workflow process for providing translational research informatics support. J Biomed Inform 42: 377–381.

Hautzinger M, Kühner C, Keller F (2009): BDI-II Beck-Depressions-Inventar: Pearson Assessment & Information GmbH. Frankfurt: Pearson Assessment.

Hayes DJ, Lipsman N, Chen DQ, Woodside DB, Davis KD, Lozano AM, Hodaie M (2015): Subcallosal cingulate connectivity in anorexia nervosa patients differs from healthy controls: A multi-tensor tractography study. Brain Stimul 8:758–768.

Heiervang E, Behrens TEJ, Mackay CE, Robson MD, Johansen-Berg H (2006): Between session reproducibility and between subject variability of diffusion MR and tractography measures. Neuroimage 33:867–877.

Jbabdi S, Johansen-Berg H (2011): Tractography: Where do we go from here? Brain Connect 1:169–183.

Jbabdi S, Woolrich MW, Andersson JLR, Behrens TEJ (2007): A Bayesian framework for global tractography. Neuroimage 37: 116–129.

Jones DK, Cercignani M (2010): Twenty-five pitfalls in the analysis of diffusion MRI data. NMR Biomed 23:803–820.

Jones DK, Knösche TR, Turner R (2013): White matter integrity, fiber count, and other fallacies: The do's and don'ts of diffusion MRI. Neuroimage 73:239–254.

Kazlouski D, Rollin MD, Tregellas J, Shott ME, Jappe LM, Hagman JO, Pryor T, Yang TT, Frank GK (2011): Altered fimbria-fornix white matter integrity in anorexia nervosa predicts harm avoidance. Psychiatry Res 192:109–116.

King JA, Geisler D, Ritschel F, Boehm I, Seidel M, Roschinski B, Soltwedel L, Zwipp J, Pfuhl G, Marxen M, Roessner V, Ehrlich S (2015): Global cortical thinning in acute anorexia nervosa normalizes following long-term weight restoration. Biol Psychiatry 77:624–632.

Kromeyer-Hauschild K, Wabitsch M, Kunze D, Geller D, Geiss HC, Hesse V, Hippel A, von J, Johnsen U, Korte DW, Menner K, Müller G, Müller JM, Niemann-Pilatus A, Remer T, Schaefer F, Wittchen HU, Zabransky S, Zellner K, Ziegler A, Hebebrand J (2001): Perzentile für den Body Mass Index für das Kindes- und Jugendalter unter Heranziehung verschiedener deutscher Stichproben. Monatsschr Kinderheilkunde 149: 807–818.

Lacey JH, Crisp AH, Hart G, Kirkwood BA (1979): Weight and skeletal maturation - a study of radiological and chronological age in an anorexia nervosa population. Postgrad Med J 55: 381–385.

Lang K, Stahl D, Espie J, Treasure J, Tchanturia K (2014): Set shifting in children and adolescents with anorexia nervosa: An exploratory systematic review and meta-analysis. Int J Eat Disord 47:394–399.

Lavagnino L, Amianto F, Mwangi B, D'Agata F, Spalatro A, Zunta-Soares GB, Daga GA, Mortara P, Fassino S, Soares JC (2015): Identifying neuroanatomical signatures of anorexia nervosa: A multivariate machine learning approach. Psychol Med 45:2805–2812.

Lebel C, Walker L, Leemans A, Phillips L, Beaulieu C (2008): Microstructural maturation of the human brain from childhood to adulthood. Neuroimage 40:1044–1055.

Le Bihan D (2003): Looking into the functional architecture of the brain with diffusion MRI. Nat Rev Neurosci 4:469–480.

Lee S, Ran Kim K, Ku J, Lee JH, Namkoong K, Jung YC (2014): Resting-state synchrony betweenanterior cingulate cortex and precuneus relates to body shape concern in anorexia nervosa and bulimia nervosa. Psychiatry Res 221:43–48.

Lerch JP, Yiu AP, Martinez-Canabal A, Pekar T, Bohbot VD, Frankland PW, Henkelman RM, Josselyn SA, Sled JG (2011): Maze training in mice induces MRI-detectable brain shape changes specific to the type of learning. Neuroimage 54: 2086–2095.

Leuven E, Sianesi B (2003): psmatch2: Stata module to perform full Mahalanobis and propensity score matching, common

support graphing, and covariate imbalance testing. Boston College Department of Economics.
Lopez C, Stahl D, Tchanturia K (2010): Estimated intelligence quotient in anorexia nervosa: A systematic review and meta-analysis of the literature. Ann Gen Psychiatry 9:40.
Mangin J-F, Fillard P, Cointepas Y, Le Bihan D, Frouin V, Poupon C (2013): Toward global tractography. Neuroimage 80:290–296.
Marshn R, Stefan M, Bansal R, Hao X, Walsh BT, Peterson BS. (2015): Anatomical characteristics of the cerebral surface in bulimia nervosa. Biol. Psychiatry 77:616–623. doi:10.1016/j.biopsych.2013.07.017.
Martin Monzon B, Hay P, Foroughi N, Touyz S (2016): White matter alterations in anorexia nervosa: Asystematic review of diffusion tensor imaging studies. World J Psychiatry 6:177–186.
Maximov II, Thonnessen H, Konrad K, Amort L, Neuner I, Shah NJ (2015): Statistical instability of tbss analysis based on dti fitting algorithm. J Neuroimaging 25:883–891.
Muetzel RL, Mous SE, van der Ende J, Blanken LM, van der Lugt A, Jaddoe VW, Verhulst FC, Tiemeier H, White T (2015): White matter integrity and cognitive performance in school-age children: A population-based neuroimaging study. Neuroimage 119:119–128.
Nagahara Y, Nakamae T, Nishizawa S, Mizuhara Y, Moritoki Y, Wada Y, Sakai Y, Yamashita T, Narumoto J, Miyata J, Yamada K, Fukui K (2014): A tract-based spatial statistics study in anorexia nervosa: Abnormality in the fornix and the cerebellum. Prog Neuropsychopharmacol Biol Psychiatry 51:72–77.
Papadopoulos FC, Ekbom A, Brandt L, Ekselius L (2009): Excess mortality, causes of death and prognostic factors in anorexia nervosa. Br J Psychiatry 194:10–17.
Parker GJ, Stephan KE, Barker GJ, Rowe JB, MacManus DG, Wheeler-Kingshott CA, Ciccarelli O, Passingham RE, Spinks RL, Lemon RN, Turner R (2002): Initial demonstration of in vivo tracing of axonal projections in the macaque brain and comparison with the human brain using diffusion tensor imaging and fast marching tractography. Neuroimage 15:797–809.
Paul TTA (2005): Eating Disorder Inventory-2 (EDI-2). Göttingen: Hogrefe. 48 p.
Petermann F, Daseking M (2009): Fallbuch HAWIK-IV. Göttingen: Hogrefe.
Pozo J, Argente J (2002): Delayed puberty in chronic illness. Best Pract Res Clin Endocrinol Metab 16:73–90.
Reyes-Haro D, Labrada-Moncada FE, Miledi R, Martínez-Torres A (2015): Dehydration-induced anorexia reduces astrocyte density in the rat corpus callosum. Neural Plast 2015: 474917.
Roberto CA, Mayer LE, Brickman AM, Barnes A, Muraskin J, Yeung LK, Steffener J, Sy M, Hirsch J, Stern Y, Walsh BT (2011): Brain tissue volume changes following weight gain in adults with anorexia nervosa. Int J Eat Disord 44:406–411.
Sarrar L, Ehrlich S, Merle JV, Pfeiffer E, Lehmkuhl U, Schneider N (2011): Cognitive flexibility and Agouti-related protein in adolescent patients with anorexia nervosa. Psychoneuroendocrinology 36:1396–1406.
Schmahmann JD, Pandya DN, Wang R, Dai G, D'Arceuil HE, de Crespigny AJ, Wedeen VJ (2007): Association fibre pathways of the brain: Parallel observations from diffusion spectrum imaging and autoradiography. Brain 130:630–653.
Schmithorst VJ, Wilke M, Dardzinski BJ, Holland SK (2005): Cognitive functions correlate with white matter architecture in a normal pediatric population: A diffusion tensor MRI study. Hum Brain Mapp 26:139–147.
Schölkopf B, Smola AJ (2002): Learning With Kernels: Support Vector Machines, Regularization, Optimization, and Beyond. Cambridge: MIT Press.
Seitz J, Buhren K, von Polier GG, Heussen N, Herpertz-Dahlmann B, Konrad K (2014): Morphological changes in the brain of acutely ill and weight-recovered patients with anorexia nervosa. A meta-analysis and qualitative review. Z Kinder Jugendpsychiatr Psychother 42:7–17.
Seitz J, Walter M, Mainz V, Herpertz-Dahlmann B, Konrad K, von Polier G (2015): Brain volume reduction predicts weight development in adolescent patients with anorexia nervosa. J Psychiatr Res 68:228–237.
Seitz J, Herpertz-Dahlmann B, Konrad K (2016): Brain morphological changes in adolescent and adult patients with anorexia nervosa. J Neural Transm (Vienna), doi:10.1007/s00702-016-1567-9.
Shott ME, Pryor TL, Yang TT, Frank GK (2015): Greater insula white matter fiber connectivity in women recovered from anorexia nervosa. Neuropsychopharmacology 41:498–507.
Simmonds DJ, Hallquist MN, Asato M, Luna B (2014): Developmental stages and sex differences of white matter and behavioral development through adolescence: A longitudinal diffusion tensor imaging (DTI) study. Neuroimage 92:356–368.
Streitbürger D-P, Möller HE, Tittgemeyer M, Hund-Georgiadis M, Schroeter ML, Mueller K (2012): Investigating structural brain changes of dehydration using voxel-based morphometry. PLoS ONE 7:e44195.
Szczepankiewicz F, Latt J, Wirestam R, Leemans A, Sundgren P, van Westen D, Stahlberg F, Nilsson M (2013): Variability in diffusion kurtosis imaging: Impact on study design, statistical power and interpretation. Neuroimage 76:145–154.
Titova OE, Hjorth OC, Schioth HB, Brooks SJ (2013): Anorexia nervosa is linked to reduced brain structure in reward and somatosensory regions: A meta-analysis of VBM studies. BMC Psychiatry 13:110.
Travis KE, Golden NH, Feldman HM, Solomon M, Nguyen J, Mezer A, Yeatman JD, Dougherty RF. (2015): Abnormal white matter properties in adolescent girls with anorexia nervosa. Neuroimage Clin 9:648–659. doi:10.1016/j.nicl.2015.10.008.
Van den Eynde F, Suda M, Broadbent H, Guillaume S, Van den Eynde M, Steiger H, Israel M, Berlim M, Giampietro V, Simmons A, Treasure J, Campbell I, Schmidt U (2012): Structural magnetic resonance imaging in eating disorders: A systematic review of voxel-based morphometry studies. Eur Eat Disord Rev 20:94–105.
Via E, Zalesky A, Sanchez I, Forcano L, Harrison BJ, Pujol J, Fernandez-Aranda F, Menchon JM, Soriano-Mas C, Cardoner N, Fornito A (2014): Disruption of brain white matter microstructure in women with anorexia nervosa. J Psychiatry Neurosci 39:367–375.
Vogel K, Timmers I, Kumar V, Nickl-Jockschat T, Bastiani M, Roebroek A, Herpertz-Dahlmann B, Konrad K, Goebel R, Seitz J (2016): White matter microstructural changes in adolescent anorexia nervosa including an exploratory longitudinal study. Neuroimage Clin 11:614–621.
von Aster M, Neubauer AC, Horn R (2006): WIE - Wechsler Intelligenztest für Erwachsene. Bern: Huber.
Wagner A, Greer P, Bailer UF, Frank GK, Henry SE, Putnam K, Meltzer CC, Ziolko SK, Hoge J, McConaha C, Kaye WH (2006): Normal brain tissue volumes after long-term recovery in anorexia and bulimia nervosa. Biol Psychiatry 59:291–293.
White T, Schmidt M, Karatekin C (2009): White matter 'potholes' in early-onset schizophrenia: A new approach to evaluate

white matter microstructure using diffusion tensor imaging. Psychiatry Res 174:110–115.

Yau WY, Bischoff-Grethe A, Theilmann RJ, Torres L, Wagner A, Kaye WH, Fennema-Notestine C (2013): Alterations in white matter microstructure in women recovered from anorexia nervosa. Int J Eat Disord 46:701–708.

Yeatman JD, Dougherty RF, Myall NJ, Wandell BA, Feldman HM (2012): Tract profiles of white matter properties: Automating fiber-tract quantification. PLoS One 7:e49790.

Yendiki A, Panneck P, Srinivasan P, Stevens A, Zollei L, Augustinack J, Wang R, Salat D, Ehrlich S, Behrens T, Jbabdi S, Gollub R, Fischl B (2011): Automated probabilistic reconstruction of white-matter pathways in health and disease using an atlas of the underlying anatomy. Front Neuroinform 5:23.

Yendiki A, Koldewyn K, Kakunoori S, Kanwisher N, Fischl B (2013): Spurious group differences due to head motion in a diffusion MRI study. Neuroimage 88C:79–90.